Quantized charge pump of massive Dirac electrons

Jun Wang and Jun-Feng Liu*
Department of Physics, Southeast University, Nanjing 210096, China
and Department of Physics, South University of Science and Technology of China, Shenzhen 518055, China
(Received 6 December 2016; published 25 May 2017)

We study a new scheme to realize a quantized two-parameter charge pump based on massive Dirac electrons. It is shown that the two time-dependent and out-of-phase staggered potentials introduced in graphene can pump out an integer number of electrons in a pumping cycle as long as the Fermi energy resides in the effective energy gap opened by pumping potentials. The dependence of the pumped charge per mode on the pumping phase or the dynamic phase exhibits a binary alternation from $+e$ to $-e$. This quantization has a topological origin and can be accounted for by adiabatic evolution of the topologically protected interfacial state forming between the two pumping sources.

DOI: 10.1103/PhysRevB.95.205433

Quantum parametric pump [1–3] has received much attention in solid-state systems, mainly because of its potential application for realizing novel current standards [4–7], but also for characterizing many-body systems [8,9]. Usually, the quantum parametric pump is referred to as two or more time-dependent potentials out of phase triggering a dc current, and the pumped current in the adiabatic limit proved to be proportional to the geometric area circled by time-dependent parameters [3].

Finding a quantized charge pump in which an integer number of charges are pumped out ($Q = Ne$) in a pump cycle is one of the central goals in this research area, because it is expected to revolutionize the electrical metrology [4–7]. In both theoretic and experimental aspects, the Coulomb blockage effect [10–14] in quantum dot systems was demonstrated useful for realizing the pumping quantization, and multiple dots in serial connection or parallel connection [12,13] could further refine this quantization.

For the noninteracting electron system, the most celebrated quantized pump is the Thouless topological pump [15] (TTP): a one-dimensional (1D) moving potential can pump out integral charges in a cycle when the Fermi energy lies in the energy gap opened by the pumping potential. This 1D periodic system is topological and the pumped charge is equal to the topological invariant of the system. Very recently, two groups have independently observed the TTP in 1D optical superlattice systems [16,17]. The surface acoustic waves [18–22] were also demonstrated experimentally to generate a quantized charge pump; however, the underlying physics is closely related to the TTP mechanism.

For the traditional two-parameter charge pump, there was no such scheme as solid as the TTP to realize the pumping quantization that is robust against disorder and parametric sensitiveness, although many works [23–27] were dedicated to this field and some preconditions [28–30] for such quantization were found. In this work, we propose a quantized two-parameter charge pump based on massive Dirac electrons, which has a topological origin but is different from the TTP mechanism formally. By introducing two out-of-phase staggered potentials in the 2D monolayer graphene, we demonstrate that a quantized charge is generated in a pump cycle due to the adiabatic evolution of the topological interface state (TIS) [31,32] bridging between the two pumping sources.

We start from a typical two-parameter pump model schematically shown in Fig. 1, where the pumping potentials Δ_1 and Δ_2 are put onto a monolayer graphene, and the device is connected through the left or right lead with the outside world. Here, $\Delta_{1,2}$ is a time-dependent staggered lattice potential endowing the Dirac electrons with a nonzero mass term. Similar pumping devices based on graphene have been extensively studied [33] but within nonstaggered potentials, so graphene did not show any topological phase transition due to the applied pumping potentials and pumped currents were nonquantized. The lattice-version Hamiltonian of the above device is given by

$$H = H_0 + V(t), \tag{1}$$

$$H_0 = -t_n \sum_{\langle ij \rangle} C_i^\dagger C_j, \tag{2}$$

$$V(t) = \sum_i \mu_i \Delta_i(t) C_i^\dagger C_i, \tag{3}$$

where H_0 describes pristine graphene and t_n is the hopping integral between nearest-neighbor carbon sites $\langle ij \rangle$. $V(t)$ is the time-dependent term composed of two staggered potentials denoted by $\Delta_i(t)$, and $\mu_i = +(-)1$ for the ith site representing the carbon A(B) atom. $\Delta_1 = \Delta_0 \cos(\omega t)$ and $\Delta_2 = \Delta_0 \cos(\omega t + \varphi)$ are homogeneous in the finite-length L_p region, where ω is the pumping frequency, Δ_0 is the pumping strength, and φ is the pumping phase shift. The normal-graphene length between Δ_1 and Δ_2 is assumed L_0.

As is known, the staggered potential $\Delta_{1,2}$ breaking the inversion symmetry of graphene [34] can open an energy gap of Dirac electrons and the system becomes a quantum valley Hall insulator. The opposite signs of Δ_1 and Δ_2 will lead to a topologically protected TIS appearing between them sustaining a pure valley current [31,32] as illustrated in Fig. 1, although there is no boundary state for a single quantum valley Hall insulator [32,34].

*liujf@sustc.edu.cn

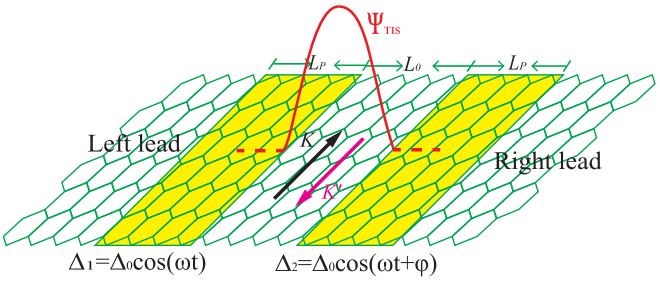

FIG. 1. Setup of a two-parameter pump device. The two pumping potentials Δ_1 and Δ_2 marked in rectangles are introduced into pristine graphene with length L_p, the distance between Δ_1 and Δ_2 is L_0, and the left and right leads connect to two unbiased electrodes. The wave function Ψ_{TIS} represents the possible in-gap topological interface state peaking in the L_0 region and attenuating in the L_p region, and sustains a valley current flowing along the transverse (y) direction.

A numerical method is first adopted to calculate the pumped current based on the BPT formula [23],

$$I_\alpha = \frac{ie}{2\pi T}\int_0^T dt\left(\frac{\partial \mathbb{S}_t}{\partial t}\mathbb{S}_t^*\right)_{\alpha\alpha}, \tag{4}$$

where $\mathbb{S}_{t\alpha\beta}$ is the instantaneous scattering matrix with $\alpha(\beta)$ being the left (right) lead index and $T = 2\pi/\omega$ is the pump cycle. Also, the zero temperature of environment (0 K) and adiabatic limit ($\omega \to 0$) are assumed in the above equation. For convenience, we use the Fisher-Lee relation [35] $\mathbb{S}_{t\alpha\beta} = -\delta_{\alpha\beta} + i\Gamma_\alpha^{1/2} G_t^r \Gamma_\beta^{1/2}$ and the Dyson equation $G_t^r = G_0^r + G_t^r V(t) G_0^r$ to rewrite the BPT formula [23] as

$$I_\alpha = \frac{e}{2\pi T}\oint dt\,\mathrm{Tr}\left[\Gamma G_t^r \dot{V} G_t^a\right]_{\alpha\alpha}, \tag{5}$$

where $\Gamma_{\alpha(\beta)}$ is the linewidth matrix of the $\alpha(\beta)$ lead and it is determined by time-independent H_0. $G_t^{r(a)} = [E \pm i0^+ - H(t)]^{-1}$ is the instantaneous retarded Green's function of the two-terminal device, $\dot{V} = dV(t)/dt$ is the time derivative of pump potentials, and the trace is over the transverse modes of the lead α.

It is assumed that our model has the translational symmetry along the y direction and the hopping integral $t_n = 1$ is set as the energy unit in numerics. In Fig. 2(a), we present the pumped current I_L flowing into the left lead as a function of the Fermi energy E. The overall current profile displays a particle-hole symmetry and fulfills the antisymmetric relationship $I_L(E) = -I_L(-E)$. For a larger pumping strength Δ_0 or longer length L_0, the pumped current shows a quantized platform ($I_L = \pm e/T$) when the Fermi energy meets $E < E_{ef} = \Delta_0/\sqrt{2}$, which is termed as the effective energy gap. For a smaller Δ_0 and L_0, the pumped current [the dotted line in Fig. 2(a)] is not quantized, although it is very sizable. The reason is the finite-size effect leading to a finite gap of the TIS [31]; therefore, either increasing the pumping strength Δ_0 or enlarging the size of pumping source L_p will significantly depress the finite gap of the TIS, so that the quantized I_L can preserve even for a negligibly small energy E.

In Fig. 2(b), we plot the k_y dependence of the pumped current $I_L(k_y)$. It is seen that the larger k_y is, the more quantized $I_L(ky)$ is. Here, the momentum k_y is counted from the Dirac

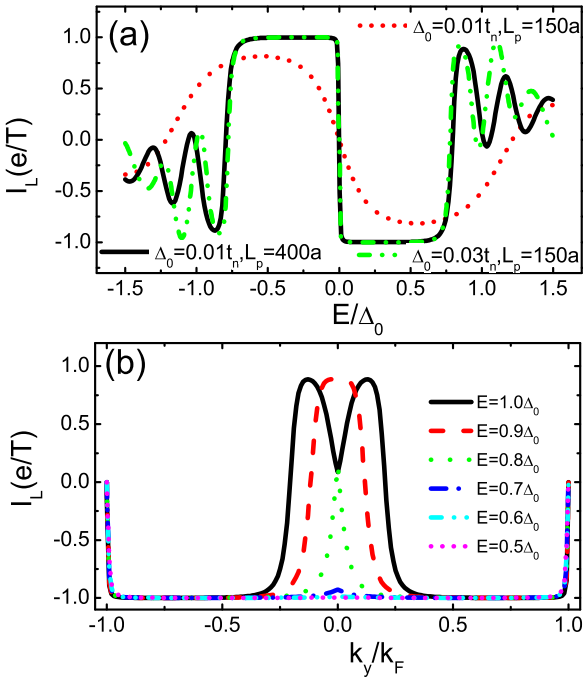

FIG. 2. Pumped current I_L as functions of (a) the Fermi energy E with $k_y = 0$ and (b) the transverse momentum k_y/k_F. a is the lattice constant and t_n is the hopping energy set as a reference of energy. Parameters are $\varphi = \pi/2$ and $L_0 = 0$.

point (K or K'), and k_F is the Fermi momentum. These results coincide with curves shown in Fig. 2(a). When the transverse momentum k_y is larger, the *propagating energy* $\mathbb{E}$ will be smaller and fulfill the condition $\mathbb{E} < E_{ef}$ more easily, so the quantization of I_L is more prone to appear, too. Even for $E \sim \Delta_0$, I_L is not quantized at $k_y = 0$ in Fig. 2(a), but it is quantized at $k_y \to k_F$ as the solid curve shown in Fig. 2(b). Therefore, the summation of $I_L(k_y)$ over k_y in the studied 2D device does not destroy the pumping quantization if $E < E_{ef}$ is valid.

In Fig. 3(a), we plot I_L versus φ within different Fermi energies E. It is clearly shown that I_L varies abruptly from positive quantized value to minus one, and it is not quantized only around $\varphi = n\pi$ (n is an integer), because the effective energy gap E_{ef} becomes too small at $\varphi \to n\pi$. Essentially, the pumped current in this two-parameter pump comes from the quantum interference effect, so the dynamic phase of electrons will inevitably affect the pumping results. In Fig. 3(b), I_L is plotted with the normal-graphene length L_0. Similarly, I_L exhibits abrupt current reversal between the two quantized values, e/T and $-e/T$. When the Fermi energy (or wave vector) is doubled, the alternating periodicity in L_0 decreases nearly by half. This confirms the effect of the dynamic phase of electrons in modulating I_L.

As we discussed earlier, the introduction of Δ_1 and Δ_2 in graphene will make the pumping source region transform into a quantum valley Hall insulator [32]; the topologically protected TIS appears between these two domains if the signs of Δ_1 and Δ_2 are opposite or vanish if they possess the same sign. The TIS appearance or disappearance in the effective energy gap

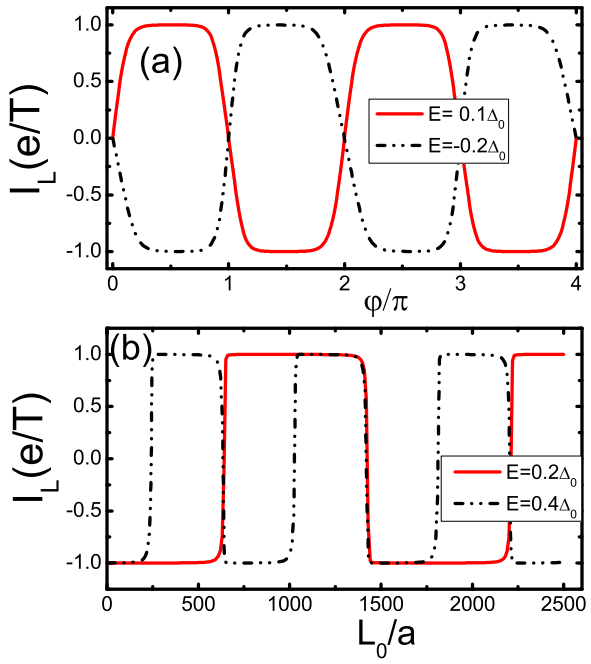

FIG. 3. Pumped current I_L as a function of (a) the pumping phase φ and (b) the length L_0. Parameters are $\Delta_0 = 0.01t_n$, $k_y = 0$, $L_0 = 0$, $\varphi = \pi/2$, and $L_p = 400a$.

seemingly makes the system experience a topological phase transition, so that a quantized pump is expected.

In Fig. 4(a), we present the instantaneous energy bands of an open device around the band center $E = 0$, where the two semi-infinite leads are omitted directly by leaving two hard

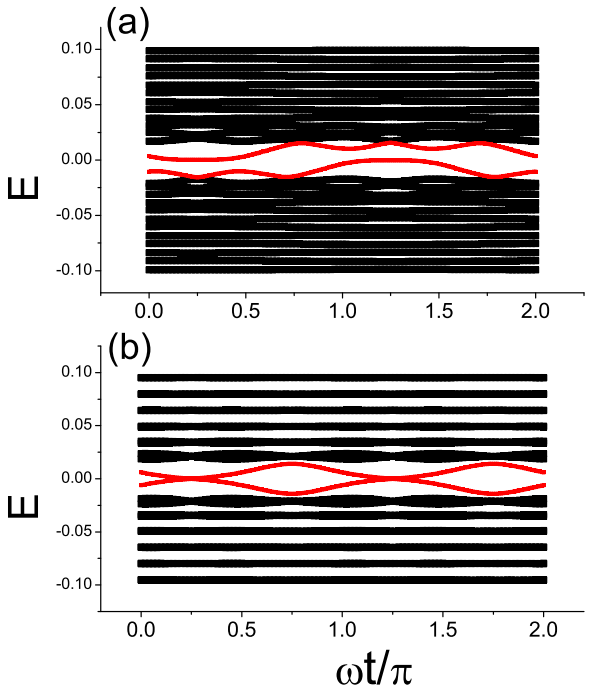

FIG. 4. Adiabatic evolution of the energy band around $E = 0$ with time ωt for (a) an open device and (b) a closed system. Two colored curves at the band center are TISs. Parameters are taken as $\varphi = \pi/2$, $L_p = 200a$, $L_0 = 0$, and $\Delta_0 = 0.02t_n$.

boundaries. One can see that a single curve either for $E > 0$ or $E < 0$ transverses the energy gap with time; this is actually the TIS evolution. Here, the TIS resides spatially between Δ_1 and Δ_2 (as illustrated in Fig. 1) but not at the two hard boundaries. When the left and right leads are connected to each other, the device forms a self-closed system, that is, there are two interfaces between Δ_1 and Δ_2. As a result, there are two TISs appearing in the energy gap (two crossings) as shown in Fig. 4(b), and each of them have the opposite chiralities.

One can assume that, in the closed system, an electron (e.g., $E = 0^+$) is residing in the TIS of the left lead (actually, shared with the right lead) at a beginning time t_0, and then at $t = t_0 + T/2$, it appears in the middle TIS localizing in the L_0 region since $\Delta_1(t_0 + T/2) = -\Delta_1(t_0)$ and $\Delta_2(t_0 + T/2) = -\Delta_2(t_0)$, and the two TISs' chiralities are reversed. At $t = t_0 + T$, this electron will come back to the TIS of the right lead. In a pump cycle T, this electron completes circling the closed device. Graf *et al.* [36] proved that the closed pumping system for the TTP is equal to the two-terminal device composed of the TTP's potential, when the device is not too short. In view of this, the TIS evolution in Fig. 4(b) can represent the quantized pumping process in an open device connected with two semi-infinite leads.

We proceed to employ a continuum model to analyze the obtained pumping quantization. It was generally argued [24–27] that when the instantaneous scattering matrix $\mathbb{S}_t$ has the formation of $\mathbb{S}_t = U(t)\tilde{\mathbb{S}}_0$ with $U(t)$ being a phase factor and $\tilde{\mathbb{S}}_0$ being independent of time, the pumped charge is quantized and equal to the winding number of $U(t)$ (up to a sign),

$$w = \frac{1}{2\pi i}\oint U^* dU. \tag{6}$$

For simplicity, we just consider a 1D continuum model describing the two-parameter pumping device in Fig. 1 as ($\hbar v_F = 1$)

$$\mathcal{H} = \sigma_x k_x + \Delta_1(t)\sigma_z\Theta_1 + \Delta_2(t)\sigma_z\Theta_2, \tag{7}$$

where $\sigma_{x,z}$ is the lattice spin operator, $\Theta_1 = \Theta(x)\Theta(L_p - x)$, and $\Theta_2 = \Theta(x - L_0 - L_p)\Theta(2L_p + L_0 - x)$ with $\Theta(x)$ being a Heaviside step function. Since I_L is focused on, we only need work out the first row of the scattering matrix $\mathbb{S}_t$, the reflection coefficient r from the left-lead injection, and the transmission coefficient t' from the right-lead injection. They are given by $r = r_1 + (t_1^2 r_2 e^{2i\varphi_0})/(1 - r_1 r_2 e^{2i\varphi_0})$, $\mathrm{t}' = t_1 t_2 e^{i\varphi_0}/(1 - r_1 r_2 e^{2i\varphi_0})$, where $r_1 = (e^{-i\theta_1} - e^{i\theta_1})/(e^{i\theta_1 + i\phi_1} - e^{-i\theta_1 - i\phi_1})$, $r_2 = e^{-2ik_0 L_p}(e^{-i\theta_2} - e^{i\theta_2})/(e^{i\theta_{1(2)} + i\phi_{1(2)}} - e^{-i\theta_{1(2)} - i\phi_{1(2)}})$, and $t_{1(2)} = e^{-ik_0 L_p}(e^{i\phi_{1(2)}} - e^{-i\phi_{1(2)}})/(e^{i\theta_{1(2)} + i\phi_{1(2)}} - e^{-i\theta_{1(2)} - i\phi_{1(2)}})$ are the reflection and transmission coefficients of the single junction consisting in a single pumping source, Δ_1 or Δ_2, respectively. Here, $e^{i\phi_{1(2)}} = (\sqrt{E + \Delta_{1(2)}} - \sqrt{E - \Delta_{1(2)}})/(\sqrt{E + \Delta_{1(2)}} + \sqrt{E - \Delta_{1(2)}})$. $k_1 = \sqrt{E^2 - \Delta_1^2}$, $k_2 = \sqrt{E^2 - \Delta_2^2}$, and $k_0 = E$ are the wave vectors in the Δ_1, Δ_2, and the normal graphene regions, respectively; while $\theta_{1,2} = k_{1,2}L_p$ and $\varphi_0 = k_0 L_0$ are correspondingly the dynamic phases of electrons.

It is seen that when either the wave vector k_1 or k_2 is imaginary ($E^2 < \Delta_1^2$ or $E^2 < \Delta_2^2$), the transmission t' of

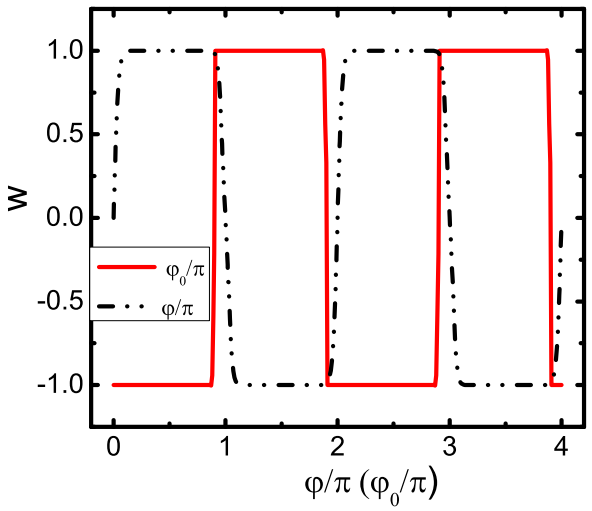

FIG. 5. Winding number (w) of the reflection coefficient versus the pumping phase φ or the dynamic phase φ_0. Parameters are $E = 0.1\Delta_0$, $\Delta_0 = 0.01t_n$, and $\varphi = \pi/2$ for the solid curve and $\varphi_0 = 0$ for the dash-dotted line.

the pumping device will decay to zero as L_p is relatively large. This means the reflection coefficient $|r| = 1$, and thus it becomes a phase factor [$r = U(t)$] in Eq. (6). Hence the pumped current I_L should be quantized, and this leads to a preposition of $\mathfrak{t}' \sim 0$ for all time t as

$$E < E_{ef} = \Delta_0\sqrt{\frac{1-\cos\varphi}{2}} \quad \left(-\frac{\pi}{2} < \varphi \leqslant \frac{\pi}{2}\right). \tag{8}$$

Here, the maximal effective energy gap E_{ef} is $\Delta_0/\sqrt{2}$ but not Δ_0 consistent with numerical results in Fig. 2(a). Figure 5 shows the winding number w of the phase $U(t)$ (=r at $E < E_{ef}$) as functions of the pumping phase φ and the dynamic phase φ_0. The curve profiles are nearly the same as the current-phase relationship of I_L shown in Fig. 3, so one can infer that the bulk states should almost not contribute to the quantized I_L, because $\mathfrak{t}' \sim 0$ is a requirement of results shown in Fig. 5. Furthermore, the quantization of numerical I_L can only come from the TIS evolution in the energy gap.

It was argued [28–30] that when there was a resonant line mostly comprised in the parameter contour circled by pumping potentials Δ_1 and Δ_2, and the device conductance keeps vanishing, the pumping would be quantized. For our model, this requirement of the quantization is always satisfied. The transmission $\mathfrak{t}'$ tends to zero for all time t on one hand, when Eq. (8) is fulfilled. On the other hand, there is always a resonant energy level appearing in the range of the smaller one of $|\Delta_1|$ and $|\Delta_2|$ and spatially residing between them, because $|\Delta_1|$ and $|\Delta_2|$ represent the instantaneous energy gaps of Dirac electrons. This resonant state is the same as the in-gap Andreev bound state appearing in a Josephson junction.

Since the TIS can be regarded as the bulk-boundary correspondence of a quantum valley Hall insulator [32], it is quite stable against moderate disorders, and this has been demonstrated in Ref. [31]. Accordingly, the quantized pump in our model is also expected to be robust against disorders, as long as the Fermi energy resides in the bulk gap opened by $\Delta_{1(2)}$ and disorders do not close this gap. This robust quantization due to topology is the same as that of the TTP, but the distinction is also obvious: our model is applicable to the 2D or 3D two-parameter charge pump, as long as the pumping potential makes the pumping-source region enter into a topological state like the charge density wave-induced insulator. Besides, the pumped current can be abruptly reversed by shifting the Fermi energy across the band center $E = 0$, or changing the pumping phase φ or the dynamic phase φ_0. Other time-dependent mass terms of Dirac electrons replacing $\Delta_{1,2}$ are expected to exert the same effect from Eq. (7). Therefore, it is convenient to control the pumping results. For instance, the quantized spin (valley) pump is possible by replacing one of $\Delta_{1,2} \sim \Delta_0\sigma_z$ with the spin (valley) dependent mass term $\Delta_0\sigma_z s_z$ ($\Delta_0\sigma_z\eta_z$), where s_z (η_z) is the spin (valley) operator. Alternatively, one can polarize the spin or valley degree of electrons in the normal graphene region between Δ_1 and Δ_2 to modulate the pumping outputs by controlling the corresponding dynamic phase φ_0.

Although the staggered potential was realized in experiment by growing graphene on the h-BN substrate [37], the bilayer graphene and monolayer silicene with a buckled lattice structure [38] are also ideal alternatives fit for our model. Especially, the TIS between opposite gate-voltage domains in the bilayer graphene was successfully observed in recent experiments [39,40]. Additionally, a time-dependent strain in graphene replacing the staggered potential can also work, because in a unitary transformation, the mass term $\Delta_0\sigma_z$ in Eq. (7) can be transformed into a uniform strain term like $\Delta_0\sigma_x$ or $\Delta_0\sigma_y$.

To conclude, we have demonstrated that the two out-of-phase staggered potentials in graphene can lead to a quantized charge pump, where each pumping potential makes the graphene insulating. The adiabatic evolution of the TIS residing between two pumping sources is responsible for this pumping quantization, and thus the quantized pump is protected by the topology. The pumping output in our model is conveniently modulated by the pumping phase, dynamic phase of electrons, and the mass type of Dirac electrons.

The work is supported by NSFC (Grants No. 11574045 and No. 11204187).

[1] B. Spivak, F. Zhou, and M. T. Beal Monod, Phys. Rev. B **51**, 13226 (1995); F. Zhou, B. Spivak, and B. L. Altshuler, Phys. Rev. Lett. **82**, 608 (1999).
[2] M. Switkes, C. M. Marcus, K. Campman, and A. C. Gossard, Science **283**, 1905 (1999).
[3] P. W. Brouwer, Phys. Rev. B **58**, R10135 (1998).
[4] Q. Niu, Phys. Rev. Lett. **64**, 1812 (1990).
[5] J. P. Pekola, O. Saira, V. F. Maisi, A. Kemppinen, M. Möttönen, Y. A. Pashkin, and D. V. Averin, Rev. Mod. Phys. **85**, 1421 (2013).

[6] M. W. Keller, A. L. Eichenberger, J. M. Martinis, and N. M. Zimmerman, Science **285**, 1706 (1999).

[7] I. M. Mills, P. J. Mohr, T. J. Quinn, B. N. Taylor, and E. R. Williams, Metrologia **43**, 227 (2006).

[8] J. Splettstoesser, M. Governale, J. König, and R. Fazio, Phys. Rev. Lett. **95**, 246803 (2005).

[9] P. Marra, R. Citro, and C. Ortix, Phys. Rev. B **91**, 125411 (2015).

[10] M. W. Keller, J. M. Martinis, and R. L. Kautz, Phys. Rev. Lett. **80**, 4530 (1998).

[11] I. L. Aleiner and A. V. Andreev, Phys. Rev. Lett. **81**, 1286 (1998).

[12] B. Kaestner, C. Leicht, V. Kashcheyevs, K. Pierz, U. Siegner, and H. W. Schumacher, Appl. Phys. Lett. **94**, 012106 (2009).

[13] M. R. Connolly, K. L. Chiu, S. P. Giblin, M. Kataoka, J. D. Fletcher, C. Chua, J. P. Griffiths, G. A. C. Jones, V. I. Fal'ko, C. G. Smith, and T. J. B. M. Janssen, Nat. Nanotechnol. **8**, 417 (2013).

[14] B. Kaestner and V. Kashcheyevs, Rep. Prog. Phys. **78**, 103901 (2015).

[15] D. J. Thouless, Phys. Rev. B **27**, 6083 (1983).

[16] M. Lohse, C. Schweizer, O. Zilberberg, M. Aidelsburger, and I. Bloch, Nat. Phys. **12**, 350 (2016).

[17] S. Nakajima, T. Tomita, S. Taie, T. Ichinose, H. Ozawa, L. Wang, M. Troyer, and Y. Takahashi, Nat. Phys. **12**, 296 (2016).

[18] J. M. Shilton, V. I. Talyanskii, M. Pepper, D. A. Ritch, J. E. F. Frost, C. J. Ford, C. G. Smith, and G. A. Jones, J. Phys.: Condens. Matter **8**, L531 (1996).

[19] P. J. Leek, M. R. Buitelaar, V. I. Talyanskii, C. G. Smith, D. Anderson, G. A. C. Jones, J. Wei, and D. H. Cobden, Phys. Rev. Lett. **95**, 256802 (2005).

[20] A. Aharony and O. Entin-Wohlman, Phys. Rev. B **65**, 241401(R) (2002).

[21] V. Kashcheyevs, A. Aharony, and O. Entin-Wohlman, Eur. Phys. J. B **39**, 385 (2004).

[22] O. Entin-Wohlman, A. Aharony, and Y. Levinson, Phys. Rev. B **65**, 195411 (2002).

[23] M. Büttiker, A. Prêre, and H. Thomas, Z. Phys. B: Condens. Matter **94**, 133 (1994).

[24] A. Andreev and A. Kamenev, Phys. Rev. Lett. **85**, 1294 (2000).

[25] J. E. Avron, A. Elgart, G. M. Graf, and L. Sadun, Phys. Rev. Lett. **87**, 236601 (2001).

[26] T. A. Shutenko, I. L. Aleiner, and B. L. Altshuler, Phys. Rev. B **61**, 10366 (2000).

[27] J. E. Avron, A. Elgart, G. M. Graf, and L. Sadun, Phys. Rev. B **62**, R10618 (2000).

[28] Y. Makhlin and A. D. Mirlin, Phys. Rev. Lett. **87**, 276803 (2001).

[29] Y. Levinson, O. Entin-Wohlman, and P. Wölfle, Physica A **302**, 335 (2001).

[30] O. Entin-Wohlman and A. Aharony, Phys. Rev. B **66**, 035329 (2002).

[31] S. K. Wang, J. Wang, and K. S. Chan, New J. Phys. **16**, 045015 (2014).

[32] M. Ezawa, Phys. Rev. B **88**, 161406(R) (2013); New J. Phys. **14**, 033003 (2012).

[33] E. Prada, P. San-Jose, and H. Schomerus, Phys. Rev. B **80**, 245414 (2009); G. M. M. Wakker and M. Blaauboer, *ibid.* **82**, 205432 (2010); R. P. Tiwari and M. Blaauboer, Appl. Phys. Lett. **97**, 243112 (2010); D. Bercioux, D. F. Urban, F. Romeo, and R. Citro, *ibid.* **101**, 122405 (2012); E. Prada, P. San-Jose, and H. Schomerus, Solid State Commun. **151**, 1065 (2011); J. Wang, K. S. Chan, and Z. Lin, Appl. Phys. Lett. **104**, 013105 (2014).

[34] D. Xiao, W. Yao, and Q. Niu, Phys. Rev. Lett. **99**, 236809 (2007).

[35] D. S. Fisher and P. A. Lee, Phys. Rev. B **23**, 6851 (1981).

[36] G. M. Graf and G. Ortelli, Phys. Rev. B **77**, 033304 (2008).

[37] R. V. Gorbachev, J. C. W. Song, G. L. Yu, A. V. Kretinin, F. Withers, Y. Cao, A. Mishchenko, I. V. Grigorieva, K. S. Novoselov, L. S. Levitov, and A. K. Geim, Science **346**, 448 (2014).

[38] P. Vogt, P. De Padova, C. Quaresima, J. Avila, E. Frantzeskakis, M. C. Asensio, A. Resta, B. Ealet, and G. Le Lay, Phys. Rev. Lett. **108**, 155501 (2012).

[39] L. Ju, Z. Shi, N. Nair, Y. Lv, C. Jin, J. Velasco Jr, C. Ojeda-Aristizabal, H. A. Bechtel, M. C. Martin, A. Zettl, J. Analytis, and F. Wang, Nature (London) **520**, 650 (2015).

[40] J. Li, K. Wang, K. J. McFaul, Z. Zern, Y. F. Ren, K. Watanabe, T. Taniguchi, Z. H. Qiao, and J. Zhu, Nat. Nanotechnol. **11**, 1060 (2011).